

Photoionization of the 3σ and 1π orbitals of CH

M.-T. Lee, J. A. Stephens, and V. McKoy

Citation: *The Journal of Chemical Physics* **92**, 536 (1990); doi: 10.1063/1.458456

View online: <http://dx.doi.org/10.1063/1.458456>

View Table of Contents: <http://scitation.aip.org/content/aip/journal/jcp/92/1?ver=pdfcov>

Published by the [AIP Publishing](#)

Articles you may be interested in

New spectroscopic data, spin-orbit functions, and global analysis of data on the $A \Sigma u + 1$ and $b \Pi u 3$ states of Na 2

J. Chem. Phys. **127**, 044301 (2007); 10.1063/1.2747595

The NaK $1(b) \Pi \Omega = 0 3$ state hyperfine structure and the $1(b) \Pi \Omega = 0 3 \sim 2(A) \Sigma + 1$ spin-orbit interaction

J. Chem. Phys. **122**, 074306 (2005); 10.1063/1.1844293

Conditions conducive to the chemi-ionization reaction $O(3P) + CH(X 2 \Pi, a 4 \Sigma -) \rightarrow HCO + (X 1 \Sigma +) + e -$

J. Chem. Phys. **115**, 6946 (2001); 10.1063/1.1405007

Spin-orbit interaction between $c 3\Sigma +$ and $B 1\Pi$ states of ScF: Effects on the fine and hyperfine structures

J. Chem. Phys. **102**, 708 (1995); 10.1063/1.469183

Spin-orbit perturbations between the $A(2)1\Sigma +$ and $b(1)3\Pi 0$ states of NaK

J. Chem. Phys. **97**, 4714 (1992); 10.1063/1.463990



AIP | APL Photonics

APL Photonics is pleased to announce
Benjamin Eggleton as its Editor-in-Chief



Photoionization of the 3σ and 1π orbitals of CH

M. -T. Lee,^{a)} J. A. Stephens, and V. McKoy

Arthur Amos Noyes Laboratory *c*, Chemical Physics, California Institute of Technology,
Pasadena, California 91125

(Received 9 August 1989; accepted 14 September 1989)

We report the results of theoretical studies of photoionization cross sections and photoelectron angular distributions for the 3σ and 1π levels of CH leading to the $A^1\Pi$, $a^3\Pi$, and $X^1\Sigma^+$ molecular ions. The calculations employed multiplet-specific Hartree-Fock potentials and numerical photoelectron continuum orbitals, obtained using the iterative Schwinger variational method. Noticeable nonstatistical behavior of the cross sections is seen for the 3σ level near threshold, although deviations are not significant at higher photon energies. A comparison with some previous theoretical studies is made.

I. INTRODUCTION

Photoionization and photodissociation processes of CH, together with the dissociative recombination of CH^+ , play an important role in modeling the relative abundances of CH^+/CH in diffuse interstellar clouds.¹⁻⁶ Due to the lack of experimentally measured cross sections for these processes, theoretical data based on *ab initio* calculations has been used for astrophysical model calculations.⁷ Our interest in CH stems mainly from its importance as a dissociation fragment or reactive intermediate species, probed, for example, by multiphoton ionization spectroscopy.^{8,9} Establishing an accurate description of the ground state photoionization dynamics of CH is therefore desirable and a useful first step.

Walker and Kelly¹ some time ago have studied the total photoionization cross sections of CH over a broad photon energy range using many-body perturbation theory. These authors predicted that the photoionization cross section of CH is nearly a factor of 2 larger than the corresponding carbon atomic value near threshold, which is quite surprising. A later calculation by Barsuhn and Nesbet² using the Stieltjes-imaging method¹⁰ and a configuration-interaction target wave function showed that the photoionization cross section near threshold was substantially smaller than that obtained by Walker and Kelly.¹ Although this disagreement can be partly attributed to electronic correlations in the target neglected in the Walker and Kelly¹ calculation, further theoretical studies are desirable in order to critically compare differences between the various sets of theoretical data and to extend them to higher photon energy.

CH is an open-shell molecule with the ground state configuration $1\sigma^2 2\sigma^2 3\sigma^2 1\pi X^2\Pi$. Ionization of a 1π electron leads to formation of the ground state $X^1\Sigma$ ion, while ionization of a 3σ electron results in the $a^3\Pi$ and $A^1\Pi$ molecular ions. In this paper we present the results of *ab initio* calculations of the photoionization cross section for the 1π and 3σ levels of CH. The continuum wave function of the photoelectron is explicitly calculated in an exact Hartree-Fock (HF) potential field of the ion. Since calculations of the asymme-

try parameters were omitted in previous theoretical studies, we present these quantities for the 3σ and 1π levels for the first time. In the present calculations, the photon energy ranges from the first ionization threshold¹¹ (IP = 10.64 eV) up to approximately 30 eV above this value. Since there are no available measured photoionization cross sections or asymmetry parameters in the literature, a comparison of our calculated cross sections is made with the theoretical results reported in earlier studies.

II. THEORY AND CALCULATIONS

The rotationally unresolved, fixed-nuclei photoionization cross section is given by

$$\sigma = \frac{4\pi^2\omega}{3c} |\langle \Psi_f(\mathbf{r}, \mathbf{R}) | \boldsymbol{\mu} | \Psi_i(\mathbf{r}, \mathbf{R}) \rangle|^2, \quad (1)$$

where $\boldsymbol{\mu}$ is the dipole moment operator and ω is the photon frequency. In Eq. (1) Ψ_i is the initial state of the molecule with N bound electrons and Ψ_f is the final ionic state plus the photoelectron. For Ψ_i we use a Hartree-Fock self-consistent field (SCF) wave function. For Ψ_f we employ the frozen-core approximation in which the bound orbitals of the ion are constrained to be identical to those of Ψ_i and the continuum photoelectron orbital hence satisfies a one-electron Schrödinger equation of the form

$$[\nabla^2 - U(\mathbf{r}, \mathbf{R}) + k^2] \phi_k(\mathbf{r}, \mathbf{R}) = \sum_i \lambda_i \chi_i, \quad (2)$$

where λ_i are Lagrange multipliers which enforce orthogonality of the continuum orbital ϕ_k to occupied orbitals χ_i , U is twice the nonlocal and nonspherical molecular ion potential, and k^2 is the photoelectron kinetic energy. Several methods for solving Eq. (2) have been developed.¹²⁻¹⁷ We solve Eq. (2) for the photoelectron orbital by the iterative Schwinger variational method, the details of which have been discussed in previous papers.^{14,15}

Calculations were done at the equilibrium internuclear distance of the ground state of CH ($R_e = 2.117$ a.u.).¹⁸ The SCF wave function for CH was obtained with a $[9s5p/5s3p]$ basis set¹⁹ augmented by two d functions ($\alpha = 0.92, 0.256$) for the carbon atom, and a hydrogen $[5s/3s]$ basis²⁰ and two p polarization functions ($\alpha = 1.4, 0.25$). With this basis, the SCF energy obtained for CH was -38.279455 a.u., in good agreement with the result obtained by Barsuhn and Nesbet²

^{a)} Permanent address: Departamento de Química, Universidade Federal de São Carlos, Caixa Postal 676, 13560 São Carlos, São Paulo, Brazil.

using an extended Slater basis set. Ionization of the 1π electron results in the ground state $X^1\Sigma^+$ ion. Ionization of a 3σ electron leads to an ionic configuration [core] $3\sigma 1\pi$, corresponding to the $a^3\Pi$ and $A^1\Pi$ states, where [core] represents the $1\sigma^2 2\sigma^2$ closed shell. For 3σ ionic states, the coupling between the photoelectron and the molecular ion results in four different continuum electronic wave functions with the symmetries $^2\Pi$, $^2\Sigma^+$, $^2\Sigma^-$, and $^2\Delta$. Here $^2\Pi$ symmetry results from $3\sigma \rightarrow k\sigma$ photoejection while all others result from $3\sigma \rightarrow k\pi$ photoejection. The $a^3\Pi$ and $A^1\Pi$ ion potentials differ in their exchange part, as defined in the one-particle Schrödinger equation

$$P \left[f_i + \sum_{\text{core}} (2J_i - K_i) + J_{3\sigma} + J_{1\pi} + a_{3\sigma} K_{3\sigma} + a_{1\pi} K_{1\pi} + \alpha S''_{1\pi} + \beta S'_{1\pi} - \epsilon \right] P |\phi_k\rangle = 0. \quad (3)$$

Here ϕ_k is a continuum orbital with a specific symmetry, J_i and K_i represent the usual Coulomb and exchange operators, P is a projection operator which ensures the orthogonality of the continuum orbital to occupied orbitals, and ϵ is photoelectron energy. The use of this projection operator is equivalent to the use of the Lagrange multipliers in Eq. (2). The S' and S'' operators are defined by^{14,15}

$$S''_{\pi} \phi_+(\mathbf{r}_1) = \phi_-(\mathbf{r}_1) \int d^3\mathbf{r}_2 [\pi_-(\mathbf{r}_2)]^* \frac{1}{r_{12}} \pi_+(\mathbf{r}_2) \quad (4a)$$

and

$$S'_{\pi} \phi_+(\mathbf{r}_1) = \pi_+(\mathbf{r}_1) \int d^3\mathbf{r}_2 [\pi_-(\mathbf{r}_2)]^* \frac{1}{r_{12}} \phi_-(\mathbf{r}_2). \quad (4b)$$

The one-electron operator f_i is

$$f_i = -\frac{1}{2}\nabla^2 - \sum_{\alpha} \frac{Z_{\alpha}}{r_{i\alpha}}, \quad (5)$$

where Z_{α} is a nuclear charge. The $a_{3\sigma}$, $a_{1\pi}$, α , and β are numerical coefficients. In the present study, the coefficients for the $3\sigma \rightarrow k\sigma$, $k\pi$ channels are identical to those reported for $5\sigma \rightarrow k\sigma$, $k\pi$ photoionization in NO.²¹ This results from the identical orbital symmetries and active electrons relevant for coupling the photoelectron to the ionic cores.

The continuum solutions of the static-exchange equations were obtained using the iterative Schwinger variational method. This procedure begins using a separable static-exchange potential of the form^{14,15}

$$U \cong \sum_{ij} \langle \mathbf{r} | U | \alpha_i \rangle [U^{-1}]_{ij} \langle \alpha_j | U | \mathbf{r}' \rangle, \quad (6)$$

where the $|\alpha_i\rangle$ are chosen to be Cartesian Gaussian functions. The basis sets used in the separable representation of the potentials here are given in Table I. The one-electron projected Schrödinger equation can be converted into an integral form, the Lippmann-Schwinger equation. Further improvement of these solutions is obtained through an iterative procedure.¹⁴ The converged solutions correspond to exact solutions of the one-electron static-exchange equation. In our calculations all relevant matrix elements and wave functions were evaluated using single-center expansions about the center of mass. For converged cross sections and asymmetry parameters, the following partial-wave expansion parameters were chosen:

TABLE I. Basis sets used in separable potential, Eq. (6).

Photoionization symmetry	Center	Type of Gaussian function ^a	Exponents
σ	C	Cartesian s	8.0,4.0,2.0,1.0,0.5,0.25
		z	1.0,0.5,0.25
	H	Cartesian s	1.2,0.4,0.1
		z	1.2,0.4,0.1
π	CM	Spherical $l = 0-3$	0.1
	C	Cartesian x	8.0,4.0,2.0,1.0,0.5,0.25
		xz	1.0,0.5,0.25
	H	Cartesian x	1.2,0.4,0.1
		xz	1.2,0.4,0.1
	CM	Spherical $l = 1-3$	0.1
δ	C	Cartesian xy	8.0,4.0,2.0,1.0,0.5,0.25
	H	Cartesian xy	1.2,0.4,0.1
	CM	Spherical $l = 2,3$	0.1

^aCartesian Gaussian basis functions are defined as $\phi^{\alpha,l,m,n,A}(\mathbf{r}) = N(x-A_x)^l (y-A_y)^m (z-A_z)^n \exp(-\alpha|\mathbf{r}-\mathbf{A}|^2)$ and spherical Gaussian functions are defined as $\phi^{\alpha,l,m,A}(\mathbf{r}) = N|\mathbf{r}-\mathbf{A}|^l \exp(-\alpha|\mathbf{r}-\mathbf{A}|^2) Y_{lm}(\Omega_{\mathbf{r}-\mathbf{A}})$. The Cartesian functions are centered on the nuclei and spherical functions are on the center of mass (CM).

- (i) maximum partial-wave expansion of the photoelectron continuum orbital = 7;
- (ii) maximum partial-wave expansion of bound orbitals in the direct potentials = 60;
- (iii) maximum partial-wave expansion of the 1σ , 2σ , 3σ , and 1π bound orbitals in the exchange potential = 20, 20, 15, and 15, respectively;
- (iv) maximum partial-wave expansion of $1/r_{12}$ in the direct and exchange terms = 40 and 20, respectively;
- (v) maximum partial-wave expansion of the nuclear potentials = 40.

The radial integration grid extended to 74 a.u. and contained 800 points. The integration step sizes ranged from 0.01 to 0.04 a.u. up to 5 a.u., and from 0.04 to 0.2 a.u. beyond this point. Only two iterations were needed to obtain converged cross sections.

III. RESULTS AND DISCUSSION

A. Photoionization of the 1π level

In Fig. 1 we show the calculated photoionization cross section for the 1π orbital of CH which leads to the formation of the ground state $X^1\Sigma^+$ ion. The enhancement of the cross section near threshold results mainly from the kinetic energy dependence of the $1\pi \rightarrow k\sigma$ channel. Examination of the eigenphase sum for this symmetry reveals that there is no shape resonance in this channel. This is not surprising since the first-row hydrides are not expected to support molecular shape resonances.²² The 1π cross sections are quite similar both in shape and magnitude to ionization from the $2p$ orbital of carbon atom,¹ which is physically reasonable.

In the same figure, the theoretical results obtained by Barsuhn and Nesbet² up to 17 eV photon energy are also shown. In general there is good agreement between these two sets of theoretical data beyond ~ 1 eV above threshold. The results obtained by Walker and Kelly¹ using the many-body

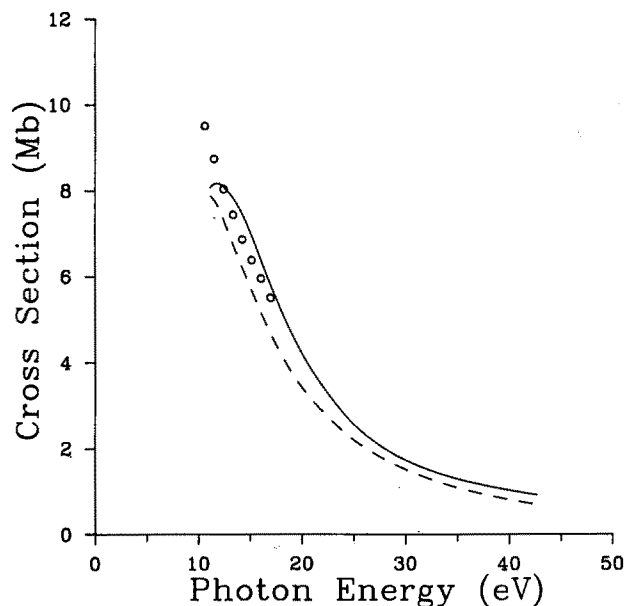


FIG. 1. Calculated photoionization cross sections for producing the $X^1\Sigma^+$ state of CH^+ . Solid line—length form; dash line—velocity form; circles—results of Barsuhn and Nesbet (Ref. 2).

perturbation theory are not shown, since these authors have only reported the total cross section. Nevertheless, for photon energies below the second ionization threshold, their corresponding cross sections for the 1π orbital are significantly larger than ours. Since our calculations were also performed using Hartree-Fock target wave functions, the good agreement between our calculated results and those of Ref. 2 suggests that electronic correlations in the initial state are not important for photoionization of the 1π level. Furthermore, there is good agreement between our calculated cross sections using the length and velocity forms of the dipole moment operator. This suggests that the observed discrepancies between the results of Refs. 1 and 2 are caused by the

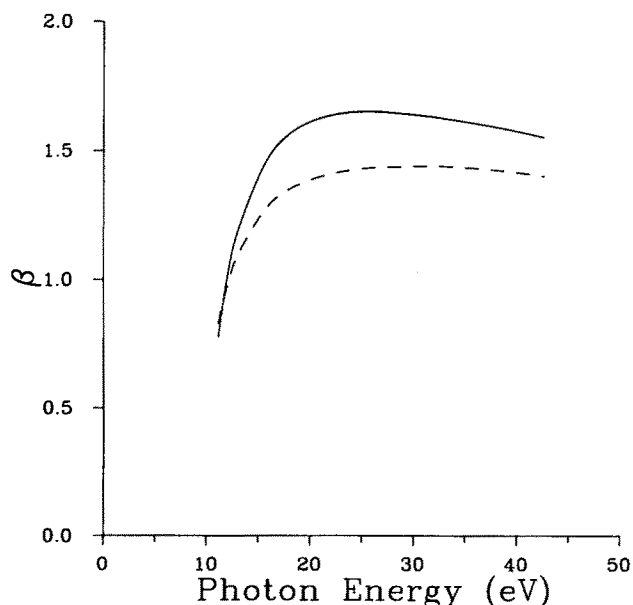


FIG. 2. Calculated asymmetry parameters for the $X^1\Sigma^+$ state of CH^+ (same designation as Fig. 1).

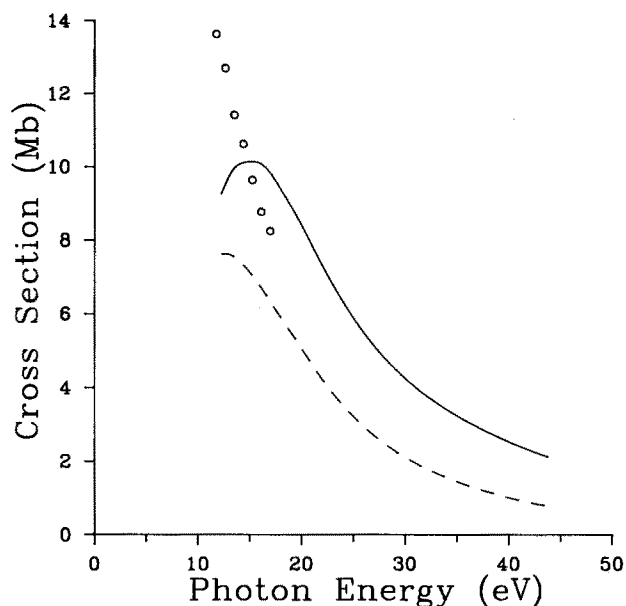


FIG. 3. Calculated photoionization cross sections for producing the $a^3\Pi$ state of CH^+ (same designation as in Fig. 1).

different theoretical approaches and convergence criterion employed.

In Fig. 2, we show the calculated asymmetry parameters β for $\text{CH } 1\pi$ photoionization. There is no available theoretical or experimental data for comparison. The asymmetry parameters obtained using the dipole length and dipole velocity forms are nearly identical at low photon energy. However, at higher photon energies, there is a difference of about 15% between these values. The variation with energy and the values of these parameters are very similar to those for $2p$ photoionization of carbon.²³ The rapid variation of β near threshold is due to variation of the s and d wave Coulomb phase shifts with photoelectron energy.²³

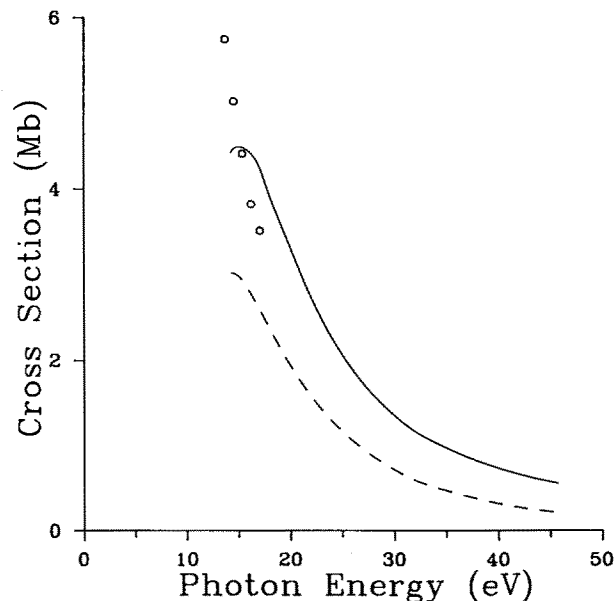


FIG. 4. Calculated photoionization cross sections for producing the $A^1\Pi$ state of CH^+ (same designation as Fig. 1).

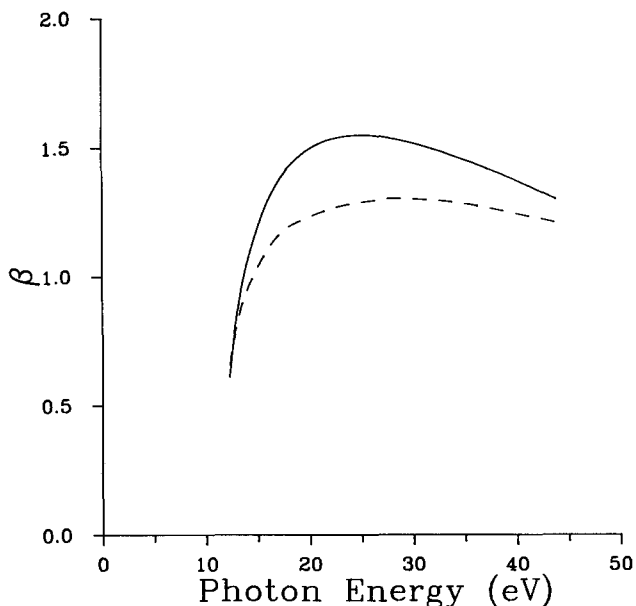


FIG. 5. Calculated asymmetry parameters for the $a^3\Pi$ state of CH^+ (same designation as Fig. 1).

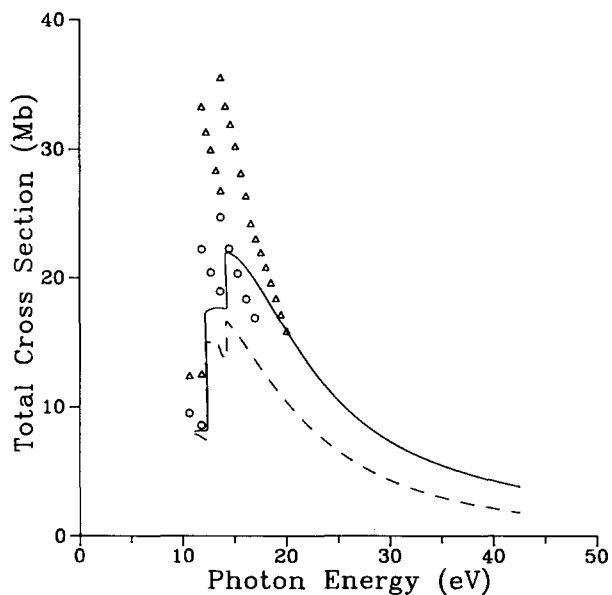


FIG. 7. Calculated total photoionization cross sections including 1π and 3σ levels (same designation as Fig. 1); triangles—results of Walker and Kelly (Ref. 1). Steps in the data occur at the 1π and 3σ ionization thresholds.

B. Photoionization of the 3σ level

Figures 3 and 4 show our calculated cross sections and angular distributions for the CH 3σ orbital, leading to the production of the $a^3\Pi$ and $A^1\Pi$ ionic states. The results of Ref. 2 for the corresponding ionic states are also shown. For reasons mentioned above, direct comparison with the calculations of Walker and Kelly¹ for these states cannot be made. As for photoionization of the 1π orbital, the enhancements near the respective thresholds are not due to shape resonances but result mainly from the energy dependences in the $3\sigma \rightarrow k\sigma, k\pi$ ionization channels. Comparison with the cross sections reported by Barsuhn and Nesbet² shows that our

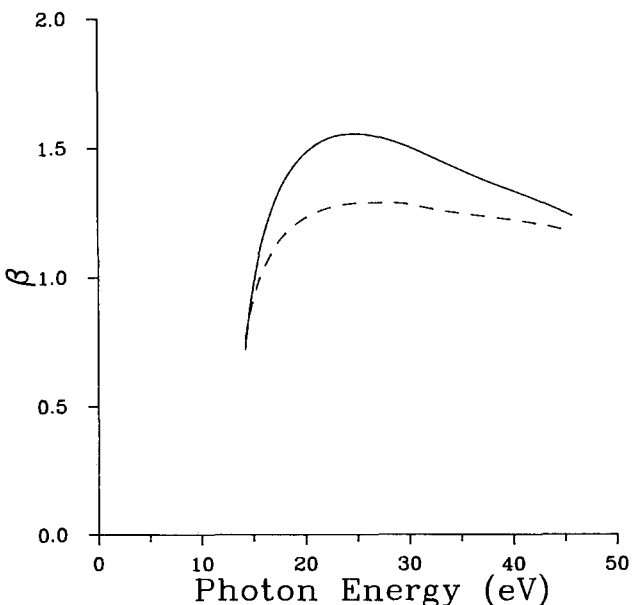


FIG. 6. Calculated asymmetry parameters for the $A^1\Pi$ state of CH^+ (same designation as Fig. 1).

results are about 20% lower for photon energies near the thresholds. However, the discrepancy diminishes rapidly with increasing photon energy, and at higher energy the results of Ref. 2 lie between our length and velocity form cross sections. The differences observed between our results and those of Ref. 2, together with the differences between the results obtained using the length and velocity form of the dipole operator, indicate that electronic correlations in the initial state are quite important. Differences up to a factor of 2 between our length and velocity results were observed in the $3\sigma \rightarrow k\sigma$ component, indicating that correlation effects are particularly important for this channel. For photon energies near threshold, where exchange is expected to be most important, we find deviations of $\sim 25\%$ from the statistical ratio of 3:1 for the cross sections leading to the $a^3\Pi$ and $A^1\Pi$ ions. However a nearly 3:1 statistical ratio is obtained at photon energies ≥ 30 eV.

In Figs. 5 and 6, we show calculated asymmetry param-

TABLE II. Photoionization cross sections and asymmetry parameters for the 1π orbital of CH. The cross sections are given in units of megabarns ($1 \text{ Mb} = 10^{-18} \text{ cm}^2$).

$h\nu(\text{eV})$	σ_L	σ_V	β_L	β_V
11.14	8.063	7.881	0.779	0.829
11.64	8.168	7.731	0.918	0.915
12.64	8.036	7.191	1.137	1.059
16.64	6.026	4.853	1.512	1.313
18.64	4.873	3.915	1.583	1.363
20.64	3.939	3.215	1.621	1.395
24.64	2.645	2.260	1.651	1.428
26.64	2.220	1.928	1.650	1.435
28.64	1.899	1.663	1.643	1.437
30.64	1.655	1.443	1.635	1.440
34.64	1.315	1.112	1.612	1.433
38.64	1.088	0.872	1.583	1.419
42.64	0.920	0.691	1.549	1.398

TABLE III. Photoionization cross sections and asymmetry parameters for the 3σ orbital of CH, producing the $A^1\Pi$ ion. The cross sections are given in units of megabarns ($1 \text{ Mb} = 10^{-18} \text{ cm}^2$).

$h\nu(\text{eV})$	σ_L	σ_V	β_L	β_V
14.18	4.421	3.023	0.718	0.757
14.68	4.490	3.002	0.895	0.871
15.68	4.461	2.869	1.115	1.008
17.68	4.009	2.439	1.350	1.150
19.68	3.387	1.993	1.468	1.223
21.68	2.803	1.618	1.528	1.262
23.68	2.317	1.319	1.552	1.282
25.68	1.930	1.083	1.551	1.289
27.68	1.624	0.891	1.534	1.289
29.68	1.380	0.735	1.507	1.283
31.68	1.184	0.606	1.472	1.267
37.68	0.830	0.379	1.366	1.231
41.68	0.669	0.276	1.306	1.209
45.68	0.555	0.209	1.236	1.174

eters corresponding to the production of the $a^3\Pi$ and $A^1\Pi$ ionic states of CH, respectively. The behavior of β for these two ionic states is very similar both in shape and magnitude, implying that the photoelectrons show essentially identical angular distribution patterns. This is in accordance with the nearly statistical ratios predicted for the cross sections. The asymmetry parameters obtained using dipole length and dipole velocity forms also show significant differences, again indicating the importance of electronic correlations in the target.

C. Total cross sections

Figure 7 shows calculated total photoionization cross sections, which correspond to the sum of the results from the 1π and 3σ levels. The comparison with the results of previous studies shows that our results agree quite well with those calculated by Barsuhn and Nesbet,² except $\sim 1\text{--}3 \text{ eV}$ above the thresholds. The total cross sections obtained by Walker and Kelly¹ are significantly larger, particularly at lower photon energies. Nevertheless, discrepancies between all calculations diminish with increasing photon energy. Comparison with results of Ref. 1 for photon energies above 20 eV cannot be made because they include contributions from the 2σ subshell, which has not been considered in the present work.

In order to facilitate the comparison of our results with future theoretical or experimental studies, Tables II–IV give values of the partial cross sections and asymmetry parameters for the 3σ and 1π levels of CH as a function of the photon energy.

ACKNOWLEDGMENTS

This work was supported by grants from the National Science Foundation (CHE-8521391), Air Force Office of Scientific Research (Contract No. 87-0039), and the Office of Health and Environmental Research of the U.S. Department of Energy (DE-FG03-87ER60513). We also acknowl-

TABLE IV. Photoionization cross sections and asymmetry parameters for the 3σ orbital of CH, producing the $a^3\Pi$ ion. The cross sections are given in units of megabarns ($1 \text{ Mb} = 10^{-18} \text{ cm}^2$).

$h\nu(\text{eV})$	σ_L	σ_V	β_L	β_V
12.28	9.255	7.627	0.609	0.655
12.78	9.604	7.631	0.790	0.775
13.78	10.038	7.483	1.019	0.925
15.78	10.121	6.846	1.273	1.091
17.78	9.497	5.993	1.413	1.188
19.78	8.538	5.157	1.489	1.228
21.78	7.449	4.316	1.530	1.261
23.78	6.439	3.593	1.547	1.282
25.78	5.581	3.001	1.549	1.294
27.78	4.879	2.524	1.537	1.304
29.78	4.306	2.144	1.520	1.301
31.78	3.834	1.834	1.498	1.297
35.78	3.103	1.362	1.442	1.278
39.78	2.551	1.022	1.375	1.245
43.78	2.118	0.773	1.300	1.209

edge use of resources of the San Diego SuperComputer Center, which is supported by the National Science Foundation. One of us (L.M.T.) thanks Fundação de Amparo a Pesquisa do Estado de São Paulo (FAPESP) for financial support and the Brazilian agency Conselho Nacional de Desenvolvimento Científico e Tecnológico (CNPq) for a research fellowship. Contribution No. 8009.

¹T. E. H. Walker and H. P. Kelly, *Chem. Phys. Lett.* **16**, 511 (1972).

²J. Barsuhn and R. K. Nesbet, *J. Chem. Phys.* **68**, 2783 (1978).

³E. F. van Dishoeck, *J. Chem. Phys.* **86**, 196 (1987).

⁴A. Giusti-Suzor and H. Lefebvre-Brion, *Astrophys. J.* **214**, L101 (1977).

⁵C. J. Williams and K. F. Freed, *J. Chem. Phys.* **85**, 2699 (1986).

⁶Note that it has also been proposed that CH^+ may be produced exothermally by shock waves in the interstellar gas. See S. R. Federman, *Astrophys. J.* **257**, 125 (1982); M. Elitzur and W. D. Watson, *ibid.* **222**, L141 (1978).

⁷A. Dalgarno and J. H. Black, *Rep. Prog. Phys.* **39**, 573 (1976).

⁸P. Chen, J. B. Pallix, W. A. Chupka, and S. D. Colson, *J. Chem. Phys.* **86**, 516 (1987).

⁹H. Rudolph, J. A. Stephens, V. McKoy, and M.-T. Lee, *J. Chem. Phys.* **91**, 1374 (1989).

¹⁰P. W. Langhoff, *Chem. Phys. Lett.* **22**, 60 (1973).

¹¹G. Herzberg and J. W. C. Johns, *Astrophys. J.* **158**, 399 (1969).

¹²W. D. Robb and L. A. Collins, *Phys. Rev. A* **22**, 2474 (1980).

¹³G. Raseev, H. Le Rouzo, and H. Lefebvre-Brion, *J. Chem. Phys.* **72**, 5701 (1980).

¹⁴R. R. Lucchese, G. Raseev, and V. McKoy, *Phys. Rev. A* **25**, 2572 (1982).

¹⁵R. R. Lucchese, K. Takasuka, and V. McKoy, *Phys. Rep.* **131**, 147 (1986).

¹⁶L. A. Collins and B. Schneider, *Phys. Rev. A* **29**, 1695 (1984).

¹⁷M. E. Smith, V. McKoy, and R. R. Lucchese, *Phys. Rev. A* **29**, 1857 (1984).

¹⁸K. P. Huber and G. Herzberg, *Molecular Spectra and Molecular Structure. Constants of Diatomic Molecules* (Van Nostrand Reinhold, New York, 1979).

¹⁹T. H. Dunning, *J. Chem. Phys.* **55**, 716 (1971).

²⁰S. Huzinaga, *J. Chem. Phys.* **42**, 1293 (1965).

²¹M. E. Smith, V. McKoy, and R. R. Lucchese, *J. Chem. Phys.* **82**, 4114 (1985).

²²J. L. Dehmer, D. Dill, and A. C. Parr, in *Photophysics and Photochemistry in the Vacuum Ultraviolet*, edited by S. McGlynn, G. Findley, and R. Huebner (Reidel, Dordrecht, 1985); p. 341.

²³S. T. Manson, *J. Elec. Spectrosc. Relat. Phenom.* **1**, 413 (1972).